

# Effect of VEGF on the Regenerative Capacity of Muscle Stem Cells in Dystrophic Skeletal Muscle

Bridget M Deasy<sup>1-4</sup>, Joseph M Feduska<sup>2</sup>, Thomas R Payne<sup>2,3</sup>, Yong Li<sup>2-5</sup>, Fabrisia Ambrosio<sup>2,6</sup> and Johnny Huard<sup>2-4,7</sup>

<sup>1</sup>Live Cell Imaging Lab, Children's Hospital of Pittsburgh of UPMC, Pittsburgh, Pennsylvania, USA; <sup>2</sup>Stem Cell Research Center, Children's Hospital of Pittsburgh of UPMC, Pittsburgh, Pennsylvania, USA; <sup>3</sup>Department of Bioengineering, University of Pittsburgh, Pittsburgh, Pennsylvania, USA; <sup>4</sup>Department of Orthopaedic Surgery, University of Pittsburgh, Pittsburgh, Pennsylvania, USA; <sup>5</sup>Laboratory of Molecular Pathology, Children's Hospital of Pittsburgh of UPMC, Pittsburgh, Pennsylvania, USA; <sup>6</sup>Department of Physical Medicine and Rehabilitation, University of Pittsburgh, Pittsburgh, Pennsylvania, USA; <sup>7</sup>Department of Microbiology and Molecular Genetics, University of Pittsburgh, Pittsburgh, Pennsylvania, USA

We have isolated a population of muscle-derived stem cells (MDSCs) that, when compared with myoblasts, display an improved regeneration capacity, exhibit better cell survival, and improve myogenesis and angiogenesis. In addition, we and others have observed that the origin of the MDSCs may reside within the blood vessel walls (endothelial cells and pericytes). Here, we investigated the role of vascular endothelial growth factor (VEGF)-mediated angiogenesis in MDSC transplantation-based skeletal muscle regeneration in *mdx* mice (an animal model of muscular dystrophy). We studied MDSC and MDSC transduced to overexpress VEGF; no differences were observed *in vitro* in terms of phenotype or myogenic differentiation. However, after *in vivo* transplantation, we observe an increase in angiogenesis and endogenous muscle regeneration as well as a reduction in muscle fibrosis in muscles transplanted with VEGF-expressing cells when compared to control cells. In contrast, we observe a significant decrease in vascularization and an increase in fibrosis in the muscles transplanted with MDSCs expressing soluble forms-like tyrosine kinase 1 (sFlt1) (VEGF-specific antagonist) when compared to control MDSCs. Our results indicate that VEGF-expressing cells do not increase the number of dystrophin-positive fibers in the injected *mdx* muscle, when compared to the control MDSCs. Together the results suggest that the transplantation of VEGF-expressing MDSCs improved skeletal muscle repair through modulation of angiogenesis, regeneration and fibrosis in the injected *mdx* skeletal muscle.

Received 18 December 2008; accepted 25 May 2009; published online 14 July 2009. doi:10.1038/mt.2009.136

## INTRODUCTION

Regenerative therapies for skeletal muscle injuries and disorders need to consider the revascularization and scarring of the tissue as well as myofiber regeneration. The use of the angiogenic factor vascular endothelial growth factor (VEGF) in gene therapy or VEGF-expressing cells in cell therapy has shown promise in a number of studies that demonstrate a role for VEGF in skin,

bone, liver, and cardiac and skeletal muscle tissue regeneration.<sup>1-4</sup> The glycoprotein VEGF is also a known mitogen for vascular endothelial cells; it stimulates angiogenesis during embryonic development, and induces vascular permeability and tumor vasculature formation.<sup>5,6</sup>

VEGF can promote both myogenesis and vascularization in a number of muscle injuries including cardiac injuries,<sup>7</sup> yet the role of VEGF in the myofiber regeneration of dystrophic muscle has not been investigated. Following ischemic injury to normal mouse skeletal tissue, VEGF expression was found to increase, and direct injection of adenovirus VEGF at the site of ischemic injury led to reduced apoptosis as compared to controls that did not receive VEGF.<sup>8</sup> Similarly, Arsic *et al.* showed that direct *in vivo* injection of VEGF complementary DNA via adeno-associated virus to injured mouse muscle (ischemic, cardiotoxic, or glycerol-induced damage) resulted in a reduction of the injured area of the muscle.<sup>9</sup>

The use of engineered myoblasts that expressed VEGF<sup>10</sup> or the use of cell types that display increased VEGF levels<sup>11</sup> showed an improvement in muscle constructs as compared to those expressing low levels of VEGF. VEGF-engineered myoblasts transplanted subcutaneously to nude mice resulted in significantly more muscle mass and higher neovascularization as compared to transplantation of myoblasts with nonfunctional protein; whereas prevascularization of tissue engineered constructs using several cell types, including mouse embryonic fibroblasts, led to increased VEGF levels and ultimately to increased survival of the muscle constructs *in vivo*.<sup>11</sup>

There are few reports on the role of VEGF in the myofiber regeneration of dystrophic muscle. VEGF coadministration was found to enhance systemic delivery of adeno-associated viral microdystrophin to skeletal muscle of *mdx* dystrophic tissue that model muscular dystrophy.<sup>12</sup> Transplantation of muscle-progenitor cells capable of sustained delivery of a functional *dys* gene have been shown to participate in the regeneration of dystrophin-positive muscle fibers of skeletal muscles of *mdx* animals.<sup>13-19</sup> We have found that muscle regeneration is mediated by muscle-derived stem cells (MDSCs) and is superior to myoblasts.<sup>18</sup> In the dystrophic skeletal muscle model, our group found that MDSCs stimulated *in vitro* with VEGF could express the endothelial protein von Willebrand factor; while *in vivo*,

Correspondence: Johnny Huard, 3460 Fifth Avenue, 4100 Rangos Research Center, Pittsburgh, Pennsylvania 15213, USA. E-mail: [jhuard@pitt.edu](mailto:jhuard@pitt.edu)

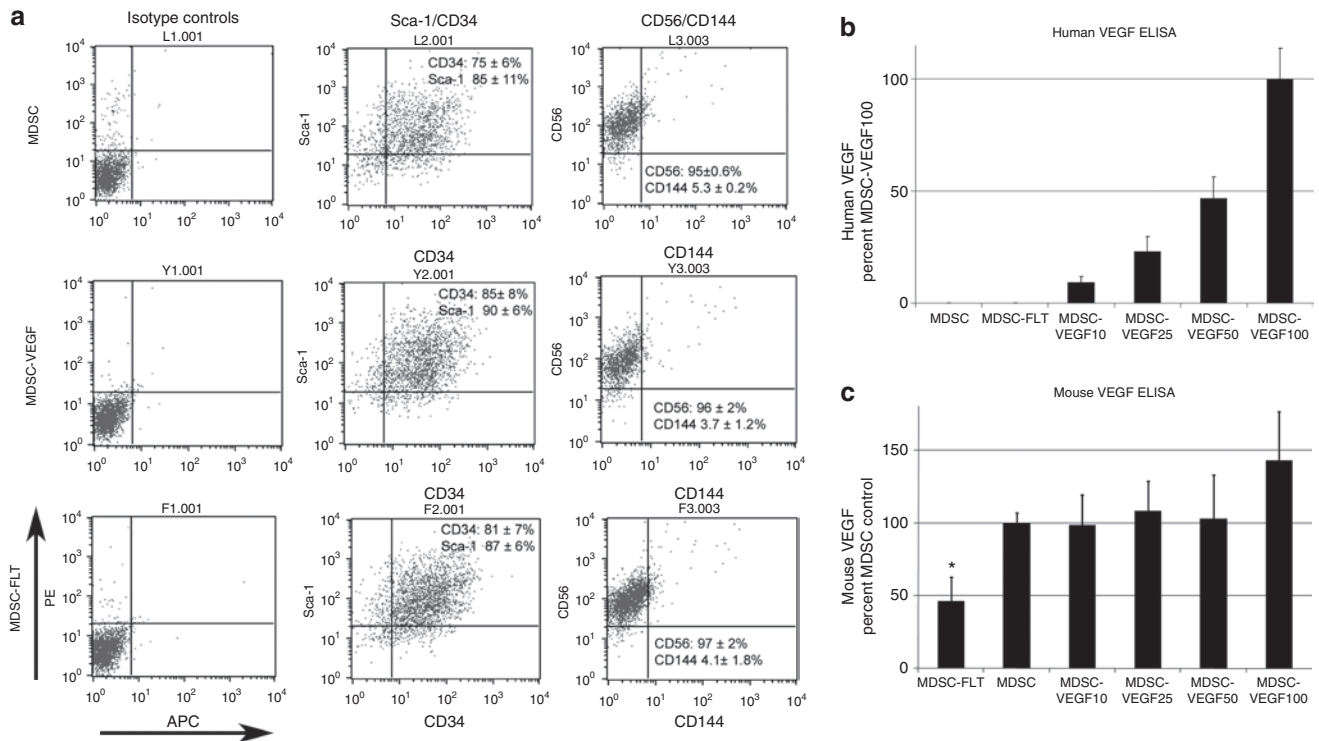


**Figure 1** Surface marker phenotype is preserved after transduction with VEGF or sFlt1, and secretion of VEGF is predictable based on the dilution factor. MDSCs were transduced to express VEGF to increase paracrine signaling of VEGF (MDSC-VEGF), or transduced with the soluble VEGF receptor, sFlt1 to reduce VEGF paracrine signaling (MDSC-FLT). (a) Representative flow cytometry dot plots show that transduction of MDSC does not significantly alter the cells' expression of stem cell markers CD34 and Sca-1, or the myogenic marker CD56. In addition, the low level of VE-cadherin (CD144) expression is not changed after transduction ( $P > 0.05$ , ANOVA,  $N = 3$ ). We examined (b) human VEGF and (c) mouse VEGF secretion in the culture media of control MDSC populations, and in populations with various amounts of VEGF-transduced cells, and in MDSC-FLT. The MDSC control population was mixed at various dilutions with VEGF-transduced cells to obtain populations that were labeled, respectively, MDSC-VEGF100 (100% MDSC-VEGF), MDSC-VEGF50 (50% MDSC and 50% MDSC-VEGF), MDSC-VEGF25 (75% MDSC and 25% MDSC-VEGF), and MDSC-VEGF10 (90% MDSC and 10% MDSC-VEGF). ELISA analysis confirmed that the level of human VEGF secretion was proportional to the amount of VEGF-transduced cells that were in the population. In addition, the amount of mouse VEGF detected in the culture media was significantly reduced for the MDSC-FLT population ( $P < 0.05$ , ANOVA). Shown are mean  $\pm$  SD. ANOVA, analysis of variance; ELISA, enzyme-linked immunosorbent assay; MDSC, muscle-derived stem cell; VE, vascular endothelial; VEGF, vascular endothelial growth factor.

donor MDSCs responded to endogenous stimuli and appeared to contribute to von Willebrand factor-positive vessels at the site of MDSC transplantation and muscle regeneration.<sup>18</sup> The group of Asahara similarly found that MDSCs could participate in vasculogenesis, neurogenesis, and myogenesis of severely damaged skeletal muscle of normal mice.<sup>20</sup>

We have already identified a role for VEGF in MDSC-mediated bone and cardiac healing. Peng *et al.* demonstrated a synergistic role for VEGF and bone morphogenic factors BMP2 and BMP4 and found that, at specific ratios, VEGF-engineered cells could enhance bone morphogenetic protein-induced endochondral bone formation and osteogenesis via increasing tissue vascularization.<sup>21,22</sup> We also found that MDSCs transplanted to ischemic cardiac tissue injury will promote functional regeneration more efficiently than more committed myoblast cells.<sup>7</sup> MDSCs exhibited a greater ability to resist oxidative stress-induced apoptosis compared to myoblasts.<sup>7</sup> MDSCs displayed greater cardiac engraftment in the infarcted hearts, induced more neoangiogenesis through graft expression of VEGF, prevented cardiac remodeling, and resulted in significant improvements in cardiac function.<sup>7,23</sup> More recently, we demonstrated that intramyocardial transplantation of MDSCs, and MDSCs that overexpress VEGF, could prevent cardiac

tissue remodeling and improve cardiac function after myocardial infarction in a mouse model as compared to hearts that were transplanted with muscle stem cells that express the soluble VEGF receptor antagonist, soluble forms-like tyrosine kinase 1 (sFlt1).<sup>23</sup>

The effects of VEGF and sFlt1 on the regenerative capacity of transplanted MDSCs in dystrophic skeletal muscle is not yet fully understood. Here, we investigated the role of VEGF secretion by transplanted MDSCs on regenerating myofibers, skeletal muscle vascularization, and fibrosis in the murine muscular dystrophy model *mdx*. To address these questions, we performed gain-and loss-of-function experiments where an *ex vivo* gene therapy approach was used through transplantation of MDSCs genetically engineered to express human VEGF, or the VEGF antagonist sFlt1, and the results were compared to control MDSCs. Our findings suggest that VEGF-expressing MDSC increase both vascularization and endogenous muscle regeneration and decreased fibrosis after implantation in dystrophic skeletal muscle.

## RESULTS

### Paracrine signaling of VEGF and its antagonist sFlt1

We transduced MDSCs with a retroviral vector encoding for human VEGF (MDSC-VEGF) or the VEGF-specific antagonist

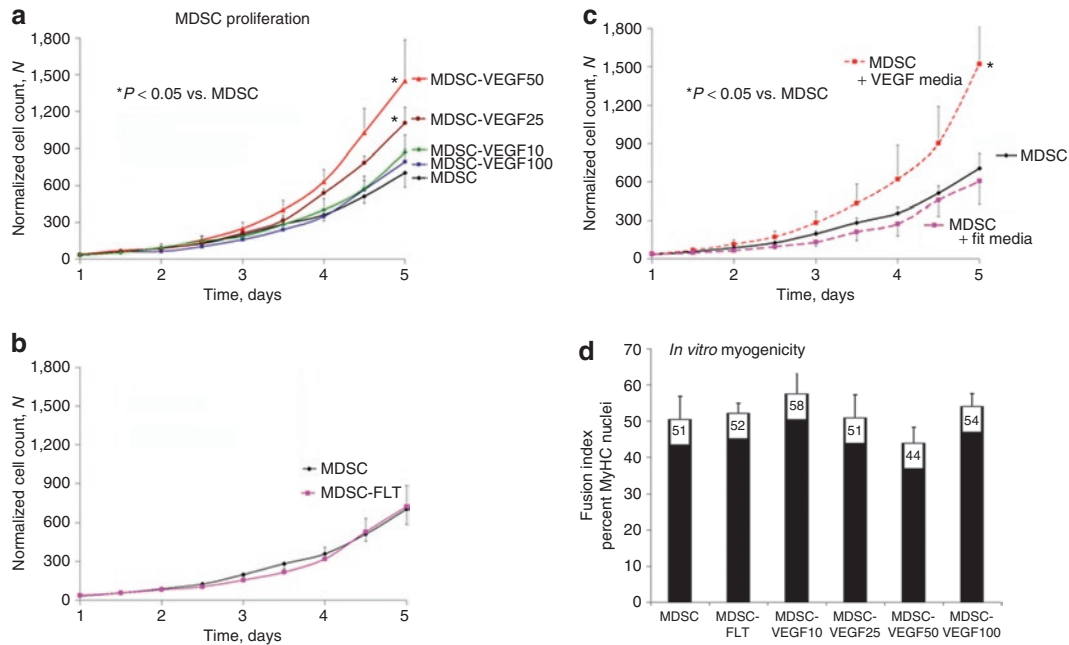


**Figure 2** VEGF increases the kinetics of cell population growth, while not affecting *in vitro* myogenic differentiation. **(a)** Proliferation kinetics show increased growth rates for MDSC-VEGF50 and MDSC-VEGF25, as compared to control MDSC ( $P < 0.05$ , *t*-test, day 5). There was no significant change in the growth rates of MDSC-VEGF100, MDSC-VEGF10, or MDSC-FLT **(b)** as compared to MDSC. **(c)** To confirm VEGF paracrine signaling, we used conditioned culture media from transduced populations (i.e., containing human VEGF or sFlt1) to examine the effect of the conditioned media on the proliferation of nontransduced populations. Nontransduced MDSC showed increased proliferation with media conditioned using MDSC-VEGF50 as compared to MDSC growth in (nonconditioned) control media. Media conditioned by MDSC-FLT cells had no effect on the proliferation rate of MDSC as compared to nonconditioned media. **(d)** The degree of myogenic differentiation was examined in the six groups as the percentage of nuclei that colocalize with myosin heavy chain expression. No significant differences were detected among the groups ( $P > 0.05$ , ANOVA). ANOVA, analysis of variance; MDSC, muscle-derived stem cell; VEGF, vascular endothelial growth factor.

soluble Flt1 (sFlt1, MDSC-FLT). To follow the fate of the injected cells, control MDSCs, as well as the MDSC-VEGF and MDSC-FLT counterpart populations, were also transduced using a retroviral vector for bacterial nuclear-localized *LacZ* (*nLacZ*). We did not detect any significant change in the expression levels of CD34, Sca1, CD56, and CD144 by flow cytometry after MDSC retrovirus transduction (Figure 1a). There was also no significant difference in the expression of the myogenic cell marker desmin, as confirmed by analysis of variance (ANOVA) [data not shown; MDSC ( $20 \pm 2\%$ ), MDSC-VEGF ( $16 \pm 2\%$ ), and MDSC-FLT1 populations ( $5 \pm 20\%$ ,  $P > 0.05$ )].

To obtain varying levels of VEGF secretion, we diluted the VEGF-transduced population with the control MDSC population, using a protocol previously described.<sup>23</sup> The following permutations of the VEGF populations were obtained: MDSC-VEGF100 (100% VEGF-transduced population), MDSC-VEGF50 (50% VEGF-transduced population + 50% MDSC), MDSC-VEGF25 (25% VEGF-transduced population + 75% MDSC), and MDSC-VEGF10 (10% VEGF-transduced population + 90% MDSC).

We subsequently measured the levels of both human and mouse VEGF that were secreted into the culture media, using species-specific enzyme-linked immunosorbent assays. As expected, we found no human VEGF in the MDSC and MDSC-FLT groups while the MDSC-VEGF100, MDSC-VEGF50, MDSC-VEGF25, and MDSC-VEGF10 groups each showed different levels of VEGF secretion (range:  $10^5$ – $10^6$  pg/ml). The level

of secreted human VEGF was proportional to their dilutions (Figure 1b): MDSC-VEGF100 ( $624 \pm 93$  ng/ml), MDSC-VEGF50 ( $293 \pm 72$  ng/ml), MDSC-VEGF25 ( $145 \pm 47$  ng/ml), and MDSC-VEGF10 ( $57 \pm 18$  ng/ml). Therefore, by diluting the VEGF-engineered cells with control cells, we could alter the dosage of VEGF secretion in the heterogeneous cell populations.

Examination of mouse VEGF expression in the populations confirmed the bioactivity of sFlt1 in the MDSC-FLT group. We observed a significant decrease in mouse VEGF in the media of MDSC-FLT cultures as compared to the control MDSC population, and as compared to all MDSC-VEGF groups [MDSC-FLT ( $98 \pm 48$  pg/ml), MDSC ( $205 \pm 54$  pg/ml), MDSC-VEGF10 ( $206 \pm 85$  pg/ml), MDSC-VEGF25 ( $217 \pm 51$  pg/ml), MDSC-VEGF50 ( $203 \pm 47$  pg/ml), and MDSC-VEGF100 ( $283 \pm 68$  pg/ml);  $P < 0.05$ , ANOVA, Figure 1c shows percent MDSC control values]. We observed no change in the intrinsic level of mouse VEGF secretion in the cells that were engineered to express human VEGF, with the exception of a significant 42% increase in mouse VEGF levels in the MDSC-VEGF100 populations as compared to the control, suggesting that some degree of autocrine VEGF signaling is also occurring (Figure 1c).

### Effect of VEGF on *in vitro* proliferation and myogenic differentiation of MDSC

We examined the effect of the various levels of VEGF on the viability and proliferation rates of the MDSCs by examining their growth over 5 days. Control MDSC, MDSC-VEGF100,

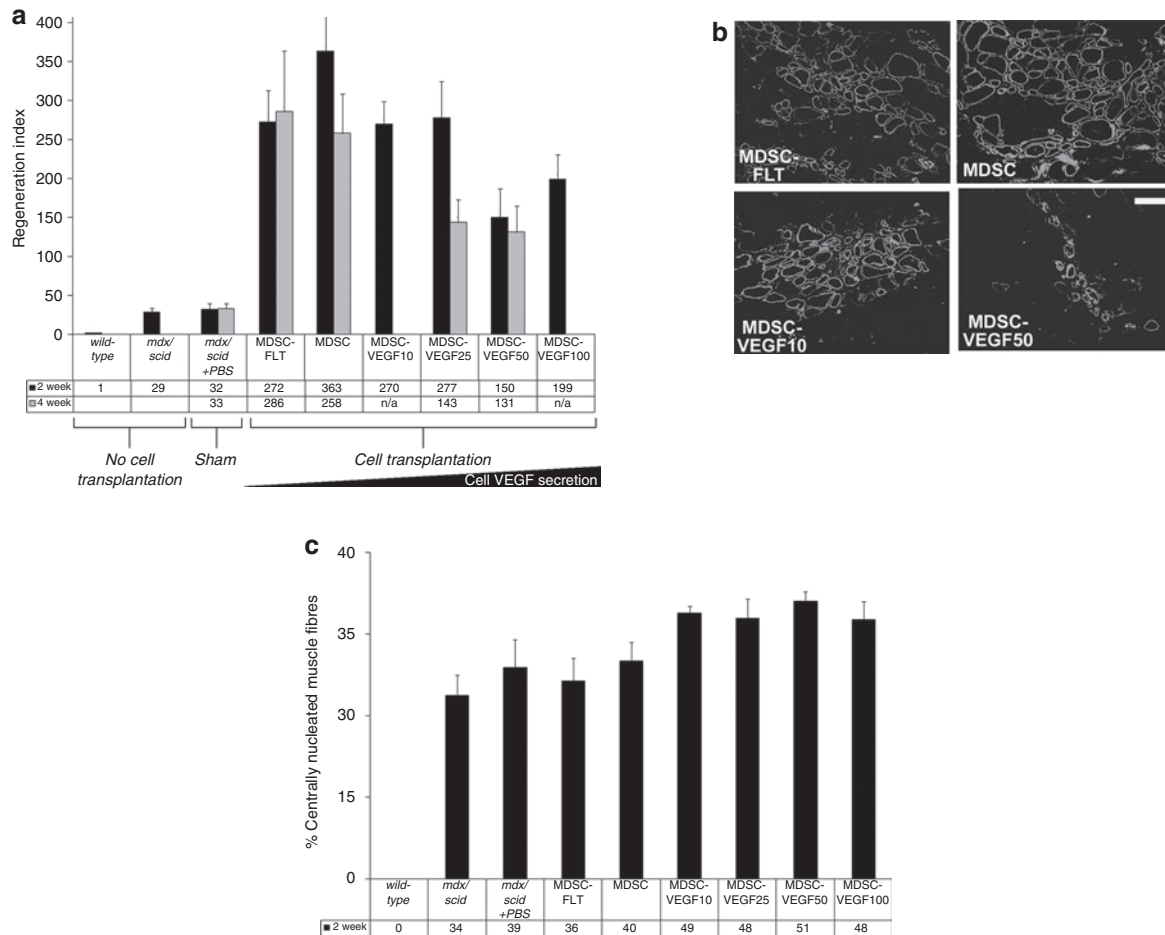


**Figure 3** *In vivo* MDSC transplantation to skeletal muscle of dystrophic tissue; restoration of dystrophin. **(a)** We used the RI (RI = number of dystrophin-positive fibers per  $10^5$  donor cells) to compare the regeneration efficiency of the different populations. We quantified the total number of dystrophin-positive fibers after transplantations of MDSCs, MDSC-FLT1 MDSC-VEGF10, MDSC-VEGF25 and MDSC-VEGF50, and MDSC-VEGF100 populations,  $N = 6$ – $16$ . Transplantation of the MDSC-VEGF50 and MDSC-VEGF100 populations resulted in significantly reduced numbers of dystrophin-positive myofibers as compared to the MDSC control. **(b)** Dystrophin immunostaining in the tissue cross-sections of gastrocnemius muscles of *mdx* mice 2 weeks post-transplantation revealed new dystrophin-positive myofibers (green) within the dystrophic animals that lack dystrophin expression (original magnification  $\times 200$ , Bar =  $100\mu\text{m}$ ). **(c)** *In vivo* examination of endogenous muscle regeneration of *mdx* tissue within  $600\mu\text{m}$  of the engraftment area of the donor cells. When injected into 8–10-week old *mdx/scid* mice, both MDSC-VEGF10 and MDSC-VEGF25 revealed significantly higher rates of centro-nucleated muscle fibers independent of the donor MDSCs, as compared to noninjected *mdx/scid* mice. While there was no evidence of a decrease in centro-nucleation between noninjured mice and the MDSC-FLT group, there was a significant difference between the disparity between the noninjected mice and VEGF10. MDSC, muscle-derived stem cell; RI, regeneration index; VEGF, vascular endothelial growth factor.

MDSC-VEGF50, MDSC-VEGF25, MDSC-VEGF10, and MDSC-FLT were cultured in a controlled bioenvironment using a live cell imaging system.<sup>24,25</sup> The resulting growth curves show significantly increased cell numbers, at day 5, for the MDSC-VEGF50 and MDSC-VEGF25 populations as compared to the control MDSC ( $P < 0.05$ , **Figure 2a**). The population with the highest level of VEGF, MDSC-VEGF100, showed population growth rates that were similar to the control MDSCs, and populations with low levels of VEGF (MDSC-VEGF10 and MDSC-FLT) also showed no significant change in proliferation as compared to the control group (**Figure 2b**). These findings suggest that specific concentrations of VEGF (MDSC-VEGF10, MDSC-VEGF25, MDSC-VEGF50) may stimulate growth in a dose-dependent manner, whereas extreme levels of VEGF (MDSC-VEGF100) does not appear to significantly influence cell growth (**Figure 2a**).

To further confirm VEGF paracrine signaling by the transduced cells (and to support the notion that *in vivo* host cells will be responsive to human VEGF secreted by the donor cells), we examined the effect of cell culture medium obtained from the VEGF-transduced cells ( $0.22\mu\text{m}$  vacuum filtered) on the proliferation of nontransduced control MDSC population (**Figure 2c**). We observed an increase in population growth when control MDSCs were cultured using media from the MDSC-VEGF50 population. In addition, nontransduced control MDSC showed no difference in proliferation using media conditioned with MDSC-FLT cells as compared to their proliferation in nonconditioned media (**Figure 2c**).

Myogenic differentiation was induced in all cell populations tested, as previously described, using a low-serum-containing medium.<sup>19,26</sup> No significant differences in the amount of myotube



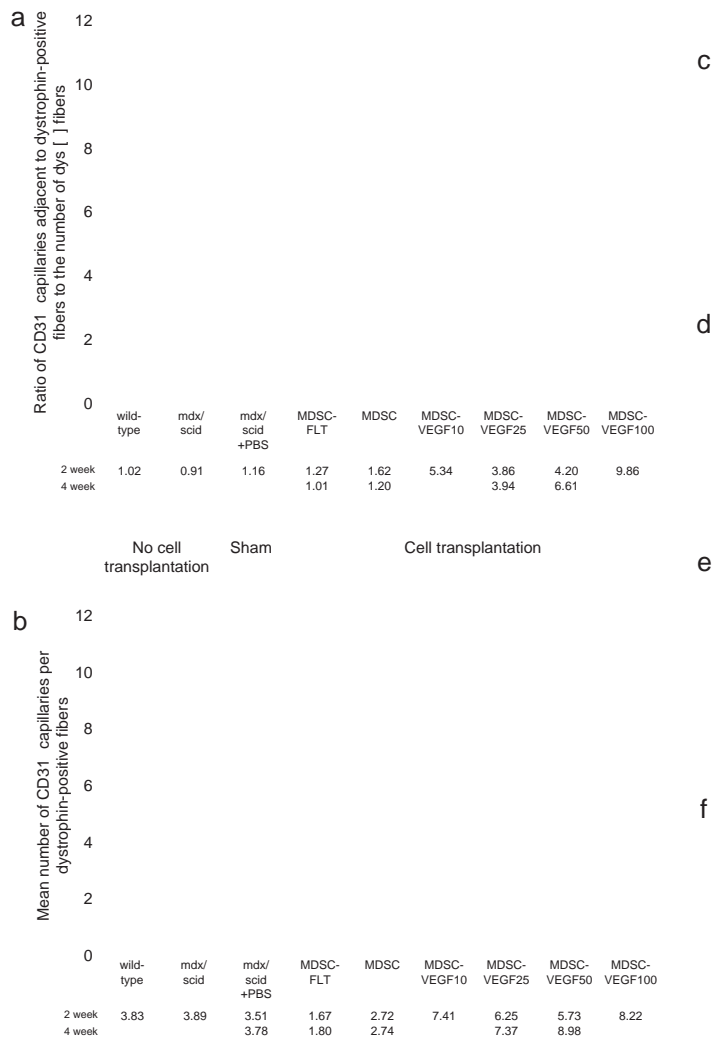


**Figure 4** Changes in vascularity associated with regenerating dystrophin-positive myofibers. **(a)** CD31 immunostaining of microvessels in the gastrocnemius muscles of *mdx* mice 2 weeks post-transplantation revealed capillaries at the site of injection. We detected significant differences in the ratio of CD31<sup>+</sup> capillaries adjacent to dystrophin-positive fibers per dystrophin-positive fiber at the site of transplantations of MDSCs as compared to MDSC-FLT1. In addition, all VEGF doses, except VEGF50, resulted in significant increases in microvascularization; MDSC-VEGF10, MDSC-VEGF25, MDSC-VEGF50, and MDSC-VEGF100 populations, *N* range from 6 to 16. **(b)** To account for tissue differences due to differences in the level of skeletal muscle regeneration, we also quantified the number of CD31<sup>+</sup> structures that were adjacent to or associated with dystrophin-positive fibers. The mean number of CD31<sup>+</sup> vessels per dystrophin fiber was significantly higher in MDSC-VEGF100, MDSC-VEGF50, MDSC-VEGF25, or MDSC-VEGF10 as compared to MDSC or MDSC-FLT. In addition, there was a significant decrease in the number of CD31<sup>+</sup> vessels as compared to MDSC-FLT ( $P < 0.01$ ). **(c-f)** CD31 (red) was colocalized with dystrophin (green) by immunofluorescent staining and quantified by examination under high power magnification ( $\times 600$ , Bar = 50  $\mu\text{m}$ ). MDSC, muscle-derived stem cell; VEGF, vascular endothelial growth factor.

formation were detected as measured by the percentage of differentiated cells that express the myosin heavy chain protein: MDSC ( $51 \pm 6\%$ ), MDSC-VEGF100 ( $54 \pm 4\%$ ), MDSC-VEGF50 ( $44 \pm 4\%$ ), MDSC-VEGF25 ( $51 \pm 6\%$ ), MDSC-VEGF10 ( $58 \pm 6\%$ ), and MDSC-FLT populations ( $52 \pm 3\%$ ,  $P > 0.05$ , ANOVA, **Figure 2d**).

### **In vivo MDSC transplantation to skeletal muscle of dystrophic muscle**

**Skeletal muscle regeneration.** We transplanted the six populations (MDSC, MDSC-FLT, MDSC-VEGF10, MDSC-VEGF25, MDSC-VEGF50, and MDSC-VEGF100) to the skeletal muscle of dystrophic and severe combined immunodeficient mice (*mdx/scid*). Two and four weeks after transplantation of the six populations, we measured the level of muscle regeneration as

the number of dystrophin-positive myofibers. We first established the baseline level of revertant dystrophin-positive fibers in the *mdx/scid* tissue. Next, we used the regeneration index (RI = number of dystrophin-positive fibers per  $10^5$  donor cells) to compare the ability of the donor cells to engraft within the host tissue. At 2 weeks post-transplantation, we quantified the total number of dystrophin-positive fibers after delivery of MDSC-FLT1 ( $272 \pm 62$ ), MDSCs ( $363 \pm 81$ ), MDSC-VEGF10 ( $270 \pm 78$ ), MDSC-VEGF25 ( $277 \pm 77$ ), MDSC-VEGF50 ( $150 \pm 47$ ), and MDSC-VEGF100 populations ( $199 \pm 31$ ,  $n = 6-16$ , mean  $\pm$  SEM, **Figure 3a**). The MDSC-VEGF50 and MDSC-VEGF100 groups had a significant difference in RI as compared to the MDSC control; transplantation of the MDSC-VEGF50 ( $P = 0.028$ ) and MDSC-VEGF100 ( $P = 0.032$ ) populations

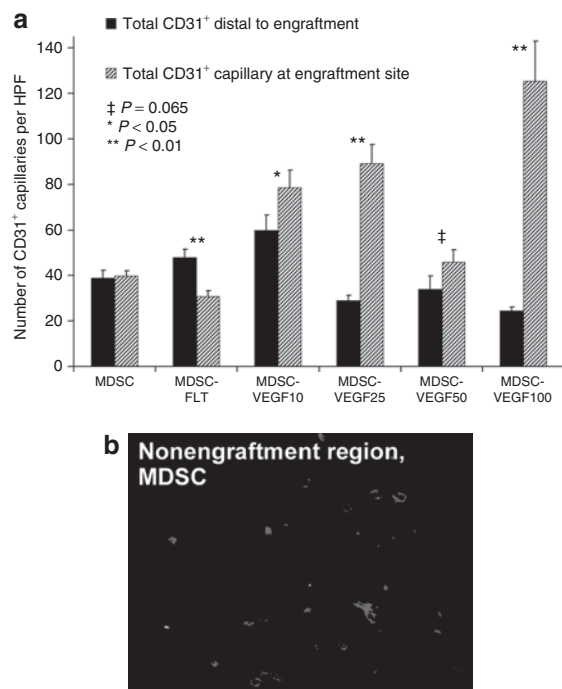


**Figure 5** Increasing VEGF secretion at engraftment site influences distal vasculature. **(a)** Microvasculature in regions distal (400–600  $\mu\text{m}$ ) to the cell injection site as compared to microvasculature at site of cell delivery was not significantly different when MDSC were transplanted ( $P = 0.453$ ,  $t$ -test,  $N = 6$ –16). However, there were significant differences in all other groups. Quantification is the total number of CD31-positive structures per high power field (HPF,  $\times 600$  or  $35 \times 10^3 \mu\text{m}^2$ ) at the site of transplantations. **(b)** Immunostaining for CD31 (red). MDSC, muscle-derived stem cell; VEGF, vascular endothelial growth factor.

resulted in a significantly reduced number of dystrophin-positive myofibers. At 4 weeks post-transplantation, we observed the highest RI with the MDSCs that were expressing endogenous or low levels of VEGF, while transplantation of cells that overexpressed VEGF showed a lower RI: MDSC-FLT1 ( $286 \pm 78$ ), MDSCs ( $258 \pm 51$ ), MDSC-VEGF25 ( $143 \pm 29$ ), and MDSC-VEGF50 populations ( $131 \pm 34$ ,  $n = 6$ –16, mean  $\pm$  SEM, **Figure 3a**). Although, there was a 25% reduction in regeneration after transplantation of MDSC-FLT as compared to MDSC, at 2 weeks, this difference was not significant. We also did not detect a significant difference in the RI of MDSC transplantations, as compared to transplantations of MDSC-VEGF25 or MDSC-VEGF50, although there were ~50% fewer dystrophin-positive fibers in these muscles. Representative dystrophin immunohistochemical stained tissue sections at 2 weeks are shown in **Figure 3b** (4 weeks not shown).

**Endogenous skeletal muscle fiber regeneration.** Central nucleation of host muscle fibers (dystrophin-negative muscle fibers) was also quantified as the percentage of host muscle fibers with centrally located nuclei (as opposed to peripheral nuclei) within a 600- $\mu\text{m}$  radial distance to the main engraftment site at 2 weeks (**Figure 3c**). As compared to noninjected *mdx/scid* muscles or muscles transplanted with sFlt-expressing cells, we observed more endogenous regeneration activity after transplantation of

VEGF-expressing cells. The number of centro-nucleated muscle fibers in noninjected *mdx/scid* ( $34 \pm 4\%$ ) increased following transplantation of each VEGF-transduced cell population; MDSC ( $40 \pm 4\%$ ), MDSC-VEGF10 ( $49 \pm 1\%$ ,  $P < 0.01$ ), MDSC-VEGF25 ( $48 \pm 4\%$ ,  $P = 0.010$ ), VEGF50 ( $51 \pm 2\%$ ,  $P < 0.01$ ), and VEGF100 ( $48 \pm 3\%$ ,  $P < 0.01$  one-tailed  $t$ -test **Figure 3c**). In addition, the four VEGF-transduced cell populations led to significantly more endogenous regeneration as compared to the MDSC-FLT population ( $36 \pm 4\%$ , all  $P < 0.05$  one-tailed  $t$ -test **Figure 3c**).

## Neovascularization

We also examined the density of capillaries in the skeletal muscle after cell transplantation. Expression of the glycoprotein adhesion receptor, CD31 (also known as platelet endothelial cell adhesion molecule 1), can provide a partial measure of the microvasculature.<sup>27,28</sup> We performed immunostaining of microvessels using CD31 antibody and colocalization with dystrophin immunostaining in the gastrocnemius muscles of *mdx/scid* mice 2 and 4 weeks post-transplantation to identify capillaries at the site of injection.

To account for tissue differences in the level of skeletal muscle regeneration, we quantified the number of CD31<sup>+</sup> structures that were adjacent to or associated with dystrophin-positive muscle fibers at the transplantation site. We quantified the ratio of CD31<sup>+</sup> structures to dystrophin-positive myofibers at the site of transplantations. We first established the similarity in the number of CD31<sup>+</sup> microvessels in wild-type C57Bl10 animals and *mdx/scid* animals (with or without phosphate buffer solution injection). On average, there was a ratio of 1.0–1.2 CD31 structures per 1 dystrophin fiber (**Figure 4a**). We detected significant differences in the amount of CD31 for transplantations of MDSCs ( $1.6 \pm 0.28$ ) as compared to MDSC-FLT1 ( $1.3 \pm 0.21$ , one-way ANOVA,  $P < 0.05$ , **Figure 4a**). In addition, all VEGF doses, at both 2 and 4 weeks, resulted in significant increases in microvascularization: MDSC-VEGF10 ( $4.4 \pm 0.79$ ), MDSC-VEGF25 ( $3.9 \pm 0.27$ ), MDSC-VEGF50 ( $4.2 \pm 0.58$ ), and MDSC-VEGF100 ( $9.9 \pm 1.9$ , one-way ANOVA,  $P < 0.05$ , **Figure 4a**).

We also quantified the mean number of CD31<sup>+</sup> structures per dystrophin-positive fiber. First, we determined that the mean number of CD31<sup>+</sup> cells per muscle fiber in wild-type animals ( $3.8 \pm 0.18$ ) and in *mdx/scid* ( $3.9 \pm 0.50$ ) muscles was not significantly different. As expected, we found that the newly regenerating dystrophin-positive fibers in muscles transplanted with nonengineered MDSCs, had fewer CD31<sup>+</sup> cells at 2 weeks ( $2.7 \pm 0.29$ ) and 4 weeks ( $2.7 \pm 0.38$ ,  $P < 0.05$ ,  $t$ -test). Overexpression of VEGF by the MDSCs at the 2-week time point resulted in significantly more CD31<sup>+</sup> cells per fiber: MDSC-VEGF10 ( $7.4 \pm 0.56$ ), MDSC-VEGF25 ( $6.2 \pm 0.58$ ), MDSC-VEGF50 ( $5.7 \pm 0.76$ ), and MDSC-VEGF100 ( $7.5 \pm 0.94$ ) (ANOVA,  $P < 0.05$ , Student Newman–Keuls test). Conversely, transplantation of MDSC-FLT cells resulted in a significant decrease in the mean number of CD31<sup>+</sup> cells per fiber ( $1.7 \pm 0.27$ ) (ANOVA,  $P < 0.05$ , Student Newman–Keuls test **Figure 4b**). Further examination of the tissue at the site of cell injection revealed that transplantation of MDSC-VEGF100 had a significantly high ratio of nuclei to muscle fiber (data not shown). This is consistent with the expectation that hemangiomas may result with large doses of VEGF

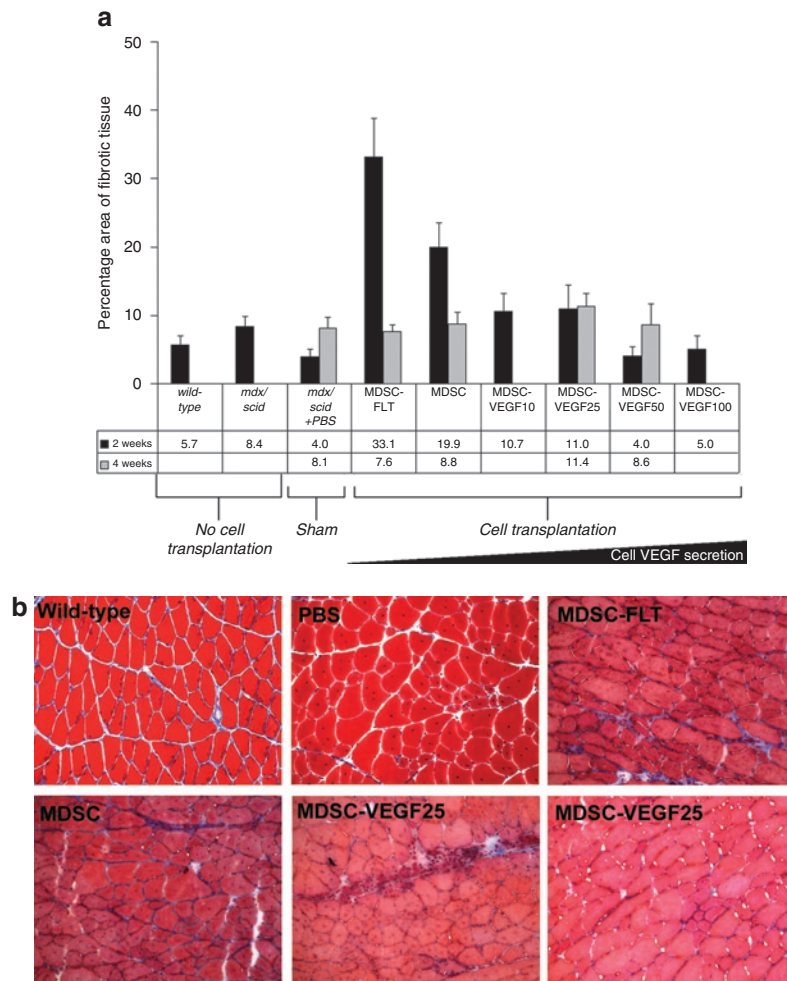


**Figure 6** Fibrosis at site of cellular transplantation. **(a)** Transplantation of MDSC, MDSC-FLT, MDSC-VEGF10, or MDSC-VEGF25 led to an increase in the amount of fibrosis as measured via trichrome staining, and as compared to noninjected tissue. The greatest amount of fibrosis occurred 2 weeks after MDSC-FLT transplantation, though fibrosis related to transplantation of these cells decreased at 4 weeks post-transplantation. Tissue that was transplanted with cells expressing VEGF (MDSC-VEGF10, MDSC-VEGF25, MDSC-VEGF50, and MDSC-VEGF100;  $N = 6-16$ ) showed less fibrosis at 2 weeks as compared to tissue transplanted with MDSC alone. By 4 weeks transplantation, there was no significant difference in the amount of fibrosis among the groups (one-way ANOVA). **(b)** Representative histological sections ( $\times 200$ , Bar = 125  $\mu\text{m}$ ). MDSC, muscle-derived stem cell; VEGF, vascular endothelial growth factor.

secretion.<sup>29</sup> All injected cell populations at the 4 week time point resulted in higher vascularization than at 2 weeks (**Figure 4b**). Representative histological sections are shown in **Figures 4c-f**. These results, taken together with the measurements of the dystrophin RI show that there is a significant positive correlation between the number of CD31<sup>+</sup> cells at the transplantation site and the skeletal muscle regeneration (dystrophin RI) in the non-engineered MDSCs, but not in the MDSC groups that overexpress VEGF, in particular at high doses (data not shown).

We also observed that the transplanted MDSC-VEGF cells were able to affect regions that were adjacent to the transplantation site. We examined microvasculature in regions distal to the cell injection site (400–600  $\mu\text{m}$  radial distance) as compared to microvasculature at site of cell delivery. We found no significant difference in these regions when MDSC were transplanted ( $P = 0.453$ ,  $t$ -test). However, there were significant differences in all other groups when we compared the microvascularization at the distal region to microvascularization at the site of cell delivery

(**Figure 5a**, 2 weeks, see figure for  $P$  values). This effect on the distal microvasculature may have been due the paracrine VEGF effect as previously described.<sup>30</sup>

### VEGF overexpressing MDSCs lead to a reduction of fibrosis

We examined the amount of fibrosis at the site of cell transplantation by assessing the relative amount of collagen. First, we observed that *mdx/scid* tissue had a larger percentage of collagenous deposition as compared to wild-type animals ( $8.4 \pm 1\%$  vs.  $5.7 \pm 1\%$ ). Transplantation of MDSC, MDSC-FLT, MDSC-VEGF10, or MDSC-VEGF25 led to an increase in the amount of fibrosis as measured via area of trichrome staining, and as compared to noninjected tissue. We observed the greatest amount of fibrosis at 2 weeks after MDSC-FLT transplantation ( $33 \pm 25\%$ ), although fibrosis related to transplantation of these cells decreased to  $8 \pm 16\%$  at 4 weeks post-transplantation (**Figure 6a**). Muscle tissue that was transplanted with cells expressing VEGF

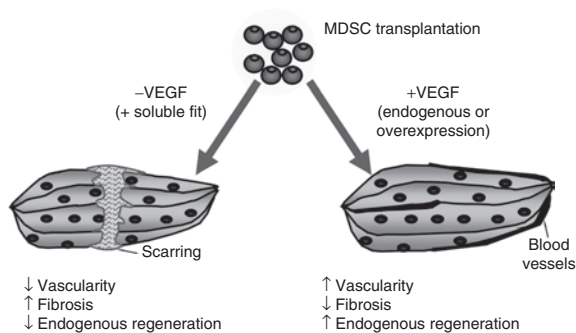


**Figure 7** Schematic representation summarizing our findings. In MDSC populations expressing increased (but low levels) of VEGF, we find decreased fibrosis, increased vascularity, increased endogenous regeneration, but decreased dystrophin RI compared to normal MDSCs. In the MDSC-FLT population, we find increased fibrosis, decreased vascularity, decreased endogenous regeneration and decreased dystrophin RI compared to normal MDSCs (but increased dystrophin RI compared to VEGF MDSCs). MDSC, muscle-derived stem cell; RI, regeneration index; VEGF, vascular endothelial growth factor.

(MDSC-VEGF10, MDSC-VEGF25, MDSC-VEGF50, and MDSC-VEGF100) showed less fibrosis at 2 weeks as compared to tissue transplanted with MDSC alone. By 4 weeks post-transplantation, there was no significant difference in the amount of fibrosis among the groups (one-way ANOVA). Representative histological sections are shown in [Figure 6b](#).

## DISCUSSION

We investigated the role of the human isoform of VEGF in MDSC-skeletal muscle regeneration in *mdx/scid* tissue. Several recent reports have shown that VEGF may play a role in skeletal muscle regeneration,<sup>8-12</sup> this study aims at examining its role in muscle stem cell-based therapy for dystrophic skeletal muscle tissue. MDSC populations have been shown to participate in skeletal muscle regeneration, in a more effective manner than myoblasts.<sup>18,31</sup> Recent reports from other investigators indicate that the vascular wall may be a source of muscle stem cells.<sup>32-34</sup> Together with our group's recent discovery that a fraction of these human muscle-derived cells also express endothelial and pericyte cell markers,<sup>34,35</sup> these results suggest that mouse MDSC may share properties with these human cells, and the mouse MDSCs may participate in angiogenesis. Here we designed gain- and loss-of-function experiments to determine whether VEGF-engineered MDSCs could improve cell-mediated muscle repair or whether reducing VEGF availability with sFlt1 would lead to a reduction in MDSC-mediated regeneration of dystrophic muscle. Our results indicate that VEGF-expressing MDSC increases both vascularization and endogenous muscle regeneration and decreased fibrosis after implantation in dystrophic skeletal muscle.

After engineering MDSC with VEGF or sFlt1, we did not observe any change in the stem cell phenotype, including no change in the expression of the endothelial cell marker vascular endothelial-cadherin (CD144). We confirmed that sFlt1 does significantly reduce the amount of bioavailable mouse VEGF in the media. Further, we found that the amount of mouse VEGF was increased in the VEGF100 group, by about 60%;

this suggests that some autocrine signaling occurs. We identified an increase in proliferation rates in some of the populations (VEGF-expressing cells). Further, we confirmed that VEGF in the media was biologically active and exerts a paracrine effect on MDSC as observed by the increase in proliferation rates of nontransduced cells. Finally, we did not observe an overall significant effect on the *in vitro* myogenic differentiation potential of the transduced MDSCs.

We next transplanted the cells to the skeletal muscles of dystrophin-deficient *mdx/scid* mice. Although there is a significant increase in the amount of CD31<sup>+</sup> cells at the site of injection of MDSC-VEGF populations, we did not observe a simultaneous increase in the number of dystrophin-positive fibers. The regeneration at both 2 weeks and 4 weeks (time points indicative of how well MDSC will regenerate dystrophin-positive fibers<sup>18,36</sup>) showed no significant change in the amount of dystrophin-positive fibers after transplantation of MDSC-VEGF100, -VEGF25, -VEGF10, or MDSC-FLT. This trend coincides with our *in vitro* myogenic indexes for the groups. Previous studies have shown that a threshold exists in the local microenvironment representing the boundary between constructive and aberrant angiogenesis when VEGF-transduced myoblasts are transplanted to normal skeletal muscle.<sup>37</sup> We similarly found that, for the VEGF50 (significant) and VEGF100 groups (not significant), there was a decrease in the number of dystrophin expressing muscle fibers ([Figure 3a](#)), and this was associated with a large increase in angiogenesis. It is interesting that transplantation of MDSC-VEGF50 consistently led to a significantly fewer number of dystrophin-positive fibers. We also found in our *in vitro* analysis that this group had the highest level of proliferation and the lowest level of myotube formation, which suggests that *in vivo* a similar dose-dependent effect may occur. Together, the *in vitro* and *in vivo* results suggest that the MDSC-VEGF50 is a highly proliferative population and these cells may not readily undergo myogenic differentiation.

To further assess muscle regeneration, we examined the percentage of muscle fibers that had recently undergone endogenous regeneration, as evident by the presence of centrally located nuclei within the dystrophin-negative fiber.<sup>38</sup> Interestingly, all VEGF groups had increases in the percentage of muscle fibers that are centrally nucleated as compared to noninjected controls, while a decrease in central nucleation was seen in MDSC-FLT groups ([Figure 3c](#)). The degeneration/regeneration cycle of *mdx* skeletal muscle fibers begins by 20 days of age, reaches its peak intensity at 60–90 days (this study), and then plateaus or diminishes beyond 90 days.<sup>39</sup> Therefore, when VEGF is overexpressed, more host fibers are actively undergoing regeneration. It is possible that the promotion of angiogenesis by the VEGF-expressing cells may occur along with activation of host stem cells and this consequently supports muscle regeneration.

We examined the vascularity in regions distal to the engraftment. For transplantations using control MDSCs we saw no difference in the amount of CD31<sup>+</sup> cells at the site of engraftment as compared to regions 400–600 μm away from the engraftment. However, in transplantations of MDSC-VEGF, we observed that when we compare the distal regions of transplantations of MDSCs to the transplantations of MDSC-VEGF, then there is a significantly reduced amount of CD31 vascularity in



these distal regions of MDSC-VEGF replicates. This is similar to previous findings indicating a reduction in capillary density in areas distal to the site of transplantation of VEGF-engineered myoblasts to *Bl/6/scid* animals.<sup>30</sup> Further, as expected, we found that there were significantly more CD31<sup>+</sup> cells at the engraftment regions than at regions that were distal to the injection of MDSC-VEGF; and there were significantly fewer CD31<sup>+</sup> cells at the engraftment regions than at regions that were distal to the injection of MDSC-FLT. These findings demonstrate the capability of VEGF secreted into the local microenvironment by donor MDSCs to affect the host vasculature at the site of cell delivery and surrounding regions.

We examined the development of fibrosis/scar tissue at the site of maximal donor cell engraftment. In studies involving cell transplantation, the needle injury that accompanies cell delivery induces the inflammatory response that ultimately leads to the development of fibrotic tissue. In the transplantations where the effects of VEGF were blocked (MDSC-FLT), the amount of fibrotic tissue at the engraftment site was significantly higher compared to the control MDSCs. Conversely, each of the VEGF cell groups significantly decreased the amount of fibrosis at the site of injection, even to the point of baseline wild-type muscle.

Several other studies support the notion that VEGF may improve graft success or bioengineering of muscle tissue. For example, Bouchentouf *et al.* showed that transplantation of GFP-myoblasts to skeletal muscle of *scid* mice engineered to overexpress VEGF led to an increase in GFP<sup>+</sup> myofibers.<sup>40</sup> Although another recent report showed that myoblasts engineered to overexpress VEGF could overcome age-related declines in myogenic activity, the VEGF-engineered myoblasts led to an increase in the size and function of the bioengineered muscle as compared to nonengineered myoblasts.<sup>41</sup> Finally, we have observed a role for VEGF in graft success of cell transplantation to cardiac tissue. We showed that transplantation of MDSCs or VEGF-expressing MDSCs, but not sFlt1-expressing MDSCs, prevents cardiac tissue remodeling and improves cardiac function after myocardial infarction in a mouse model.<sup>23</sup>

This study highlights the multifactorial process of skeletal muscle healing that would be involved following gene and cell therapies for muscular dystrophy. Several factors are involved in muscle healing including dystrophin-positive regenerating fibers, endogenous muscle regeneration, microvascularization, and level of fibrosis. Our results indicate that VEGF affects each of these aspects of the skeletal muscle regeneration process (Figure 7). The transplantation of VEGF-expressing MDSCs increased the vascularization of dystrophic tissue and the endogenous regeneration, while reducing fibrosis. When VEGF is inhibited via its soluble antagonist with the sFlt1-expressing cells, the level of angiogenesis was inhibited while increased fibrosis was observed. Together the results suggest that the transplantation of VEGF-expressing MDSCs may improve skeletal muscle repair by modulating angiogenesis, muscle fiber regeneration and fibrosis via paracrine effects on host progenitor cells by the transplanted cells. This study also highlights that evaluating the regeneration process through conventional monitoring of only dystrophin-positive muscle fibers may be insufficient to describe muscle healing, and illustrates the role of the donor cells to signal host progenitor cells for the repair process.

## MATERIALS AND METHODS

### Cell isolation, cell culture, and transduction with LacZ, VEGF, and sFlt1.

MDSCs were obtained, as previously described, from normal (C57BL/6J) newborn (1–2 day) mice.<sup>18,31</sup> MDSC were cultured in normal growth medium: Dulbecco's modified Eagle's medium supplemented with 10% fetal bovine serum, 10% horse serum, 1% penicillin/streptomycin, and 0.5% chick embryo extract (Gibco-BRL, Invitrogen, Carlsbad, CA) at an initial seeding density of 225 cells/cm<sup>2</sup> on collagen type X coated flasks. As previously described, retroviral vectors expressing human VEGF, sFlt1, or the bacterial *LacZ* gene were constructed by cloning the VEGF<sub>165</sub> complementary DNA (from InvivoGen, San Diego, CA), complementary DNA encoding human sFlt1 (from InvivoGen), or the *LacZ* gene into pCLX, resulting in pCLVEGF, pCLsFlt1, and pCLLacZ, respectively. The titer of the viral vectors was estimated to be  $5 \times 10^5$ – $2 \times 10^6$  colony-forming units/ml by limiting dilution.<sup>21</sup>

CD34, Sca-1, CD56, CD144 (vascularendothelial-cadherin) expression were analyzed by flow cytometry (FACSARIA; Becton Dickinson, San Jose, CA). MDSCs were labeled with rat anti-mouse Sca-1 (R-phycoerythrin) and anti-rat CD34 (biotin), anti-mouse CD56 PE, and anti-ms biotinylated CD144 monoclonal antibodies. A separate portion of cells was treated with equivalent amounts of isotype control antibodies. Both fractions then were washed and labeled with streptavidin–allophycocyanin. 7-Amino-actinomycin D was added to exclude nonviable cells from the analysis. A protein profile also was obtained from a nonsorted fraction of the MDSC suspension. All antibodies, streptavidin–allophycocyanin, and 7-amino-actinomycin D were obtained from BD Biosciences, San Jose, CA. Differences in the percentage of cells that expressed markers was performed using a Student's *t*-test (SigmaStat, version 2.0; Jandel Scientific; SPSS, Chicago, IL).

**Enzyme-linked immunosorbent assay for VEGF.** The levels of mouse and human VEGF (or sFlt) secreted from the transduced cells were measured using enzyme-linked immunosorbent assay kits (R&D Systems, Minneapolis, MN). Cells were plated at a density of 500,000 cells total per 2 cm<sup>2</sup>/1 ml growth medium for 24 hours. Media was removed and analyzed according to manufacturer's protocols. Statistical comparisons were performed on differences in percent secretion relative to controls using one-way ANOVA followed by Tukey's multiple comparison tests.

**Proliferation kinetics and paracrine effects of VEGF.** Time-lapsed imaging was used to measure parameters of proliferation kinetics.<sup>24,26</sup> Briefly, cell populations were plated at 225 cells/cm<sup>2</sup> and cell numbers were quantified at 6-hour intervals over a 5-day period. Population doubling rates were measured from the best fit exponential curve to the experimental data.<sup>19</sup> To confirm VEGF paracrine signaling by the transduced cells, we examined the effect of conditioned medium (supernatant from cultures) on the proliferation of nontransduced population. To obtain conditioned media, MDSC-VEGF50 and MDSC-FLT populations were grown in 20% serum Dulbecco's modified Eagle's medium for 24 hours; the supernatant media was then removed, centrifuged and labeled as conditioned media CM-VEGF and CM-FLT, respectively. Nontransduced control MDSC were then cultured in CM-VEGF and CM-FLT and proliferation kinetics were measured and compared to cells grown in (nonconditioned) control media and transduced. Statistical differences in growth rates at day 5 were as tested using a Student's *t*-test.

**In vitro myogenic differentiation.** MDSCs were plated at 1,000 cells/cm<sup>2</sup> in normal 20% serum Dulbecco's modified Eagle's medium for 3 days, and then were placed in 2% serum Dulbecco's modified Eagle's medium for an additional 4 days to induce myogenic differentiation. On day 7, immunostaining was performed to reveal fast myosin heavy chain expression. Methanol-fixed cultures were blocked with 5% horse serum and were incubated with monoclonal mouse anti-myosin heavy chain (Sigma, 1:250; Sigma Aldrich, St Louis, MO), biotinylated

immunoglobulin G (1:250, Vector), and streptavidin-Cy3 (1:500). Differentiation efficiency was calculated as the ratio of myogenic nuclei to total nuclei. Statistical differences in growth rates at day 5 were as tested using a Student's *t*-test.

**Cell transplantation, skeletal muscle regeneration, and immunohistochemistry.** The use of animals and the surgical procedures performed in this study were approved by the Institutional Animal Care and Use Committee of the Children's Hospital of Pittsburgh (University of Pittsburgh Medical Center). *Mdx/scid* mice were bred by crossing C57BL/10ScSn-Dmdmdx and C57BL/6J-Prkdcscid/SzJ mice. The individual *mdx* and *scid* strains were originally obtained from the Jackson Laboratory and then bred at the institution's animal facility.

To each muscle replicate, we transplanted  $1 \times 10^5$  cells into the gastrocnemius muscle of 8- to 10-week-old *mdx/scid* mice via a previously described process.<sup>42</sup> Two-week groups consisted of: MDSC (*n* = 16), MDSC-FLT (*n* = 16), MDSC-VEGF10 (*n* = 8), MDSC-VEGF25 (*n* = 10), MDSC-VEGF50 (*n* = 6), MDSC-VEGF100 (*n* = 6), whereas the 4-week groups consisted of MDSC (*n* = 8), MDSC-FLT (*n* = 6), MDSC-VEGF25 (*n* = 6), and MDSC-VEGF50 (*n* = 6). For diluted groups, the control MDSC and MDSC-VEGF were mixed at the given ratio immediately prior to injection. At 2 and 4 weeks after transplantation, the mice were killed and the muscles were sectioned by cryostat (10  $\mu$ m).

Tissues sections were immunostained to colocalize dystrophin and CD31. Slides were fixed with 5% neutral buffered formalin for 5 minutes, followed by a blocking solution consisting of 7.5% goat serum/7.5% donkey serum (15% total) for 1 hour. Primary antibodies were suspended in a diluted version of the blocking solution (5% horse/donkey serum) and consisted of purified rat anti-mouse CD31 (1:250; BD Biosciences, platelet endothelial cell adhesion molecule 1, cat. no. 55370; BD Biosciences), and rabbit anti-mouse dystrophin (1:300, cat. no. ab15277; Abcam, Cambridge, MA). The secondary antibody solution consisted of goat anti-rat immunoglobulin G Alexaflour 555 (cat. no. #A21434; Invitrogen/Molecular Probes, Eugene, OR) diluted in phosphate buffer solution at 1:250 to detect CD31, and donkey anti-rabbit Alexaflour 488 at 1:300 to detect dystrophin (cat. no. A21206). Hoechst solution (1  $\mu$ g/ml) was added to the secondary antibody solution for the final 5 minutes. Images were taken on a Nikon ES800 microscope with Retiga EXi Camera using Northern Eclipse software (version 6.0). Dystrophin fibers were quantified as previously described.<sup>42</sup> Angiogenesis was quantified by counting the lumen of each blood vessel (60 $\times$ ). Only the presence of capillary lumen was quantified. ANOVA was performed to determine statistically significant difference among the groups.

**Fibrosis.** Tissue sections were analyzed for fibrosis by staining for collagenous tissue with a Masson's trichrome staining kit provided by IMEB (San Marcos, CA; cat. no. K7228). This technique stains collagen blue, nuclei black, and muscle fibers and nonspecific tissue red. Appropriate thresholds were set in order to quantify the percentage of fibrotic area in the muscle cross-section.

**Image analysis.** All fluorescent and bright-field microscopy was performed at room temperature using a Nikon Eclipse E800 microscope (Nikon, Tokyo, Japan) equipped with  $\times 20/0.75$  (DIC M,  $\infty/0.17$ ) and  $\times 60/0.95$  (DIC M,  $\infty/0.11$ – $0.23$  corr) objectives and a Retiga EXi digital camera (QImaging, Surrey, Canada). No imaging medium was used, and fluorochromes used are as indicated. Images were acquired using either Northern Eclipse (version 6.0; Empix Imaging, Cheektowaga, NY) or QCapture (Suite 2.68.2, QImaging). Images were acquired at exposures based on unstained negative controls. All quantitative analysis was performed either with Northern Eclipse version 6.0 or ImageJ software (National Institute of Health, Bethesda, MD). Final figure presentations were prepared in Adobe Photoshop (version 7.0; Adobe Systems, San Jose, CA).

## ACKNOWLEDGMENTS

We thank Bruno Peault (University of Pittsburgh/Children's Hospital of Pittsburgh) for insightful discussions and Hairong Peng (University of Pittsburgh/UPMC) for the VEGF and sFlt1 constructs. This work was performed at the Stem Cell Research Center, Pittsburgh, PA, and was supported in part by grants from the National Institutes of Health (NIH R01 AR49684-01 to J.H.), US National Institutes of Arthritis and Musculoskeletal Research (R03 AR053678 to B.M.D.), the US Department of Defense (W81XWH-06-1-0406), the William F. and Jean W. Donaldson Chair at Children's Hospital of Pittsburgh, the Henry J. Mankin Chair at the University of Pittsburgh, and the Orris C. Hirtzel and Beatrice Dewey Hirtzel Memorial Foundation. J.H. serves as a consultant to Cook MyoSite, Inc. and T.R.P. is an employee of Cook MyoSite, Inc. All the other authors have no potential conflicts of interest to declare.

## REFERENCES

- Geiger, F, Bertram, H, Berger, I, Lorenz, H, Wall, O, Eckhardt, C *et al.* (2005). Vascular endothelial growth factor gene-activated matrix (VEGF165-GAM) enhances osteogenesis and angiogenesis in large segmental bone defects. *J Bone Miner Res* **20**: 2028–2035.
- Oe, H, Kaido, T, Mori, A, Onodera, H and Imamura, M (2005). Hepatocyte growth factor as well as vascular endothelial growth factor gene induction effectively promotes liver regeneration after hepatectomy in Solt-Farber rats. *Hepatogastroenterology* **52**: 1393–1397.
- Youssif, M, Shiina, H, Urakami, S, Gleason, C, Nunes, L, Igawa, M *et al.* (2005). Effect of vascular endothelial growth factor on regeneration of bladder acellular matrix graft: histologic and functional evaluation. *Urology* **66**: 201–207.
- Beraza, N, Marqués, JM, Martínez-Ansó, E, Iñiguez, M, Prieto, J and Bustos, M (2005). Interplay among cardiostrophin-1, prostaglandins, and vascular endothelial growth factor in rat liver regeneration. *Hepatology* **41**: 460–469.
- Senger, DR, Galli, SJ, Dvorak, AM, Perruzzi, CA, Harvey, VS and Dvorak, HF (1983). Tumor cells secrete a vascular permeability factor that promotes accumulation of ascites fluid. *Science* **219**: 983–985.
- Dvorak, HF (2002). Vascular permeability factor/vascular endothelial growth factor: a critical cytokine in tumor angiogenesis and a potential target for diagnosis and therapy. *J Clin Oncol* **20**: 4368–4380.
- Oshima, H, Payne, TR, Urish, KL, Sakai, T, Ling, Y, Gharaibeh, B *et al.* (2005). Differential myocardial infarct repair with muscle stem cells compared to myoblasts. *Mol Ther* **12**: 1130–1141.
- Germani, A, Di Carlo, A, Mangoni, A, Straino, S, Giacinti, C, Turrini, P *et al.* (2003). Vascular endothelial growth factor modulates skeletal myoblast function. *Am J Pathol* **163**: 1417–1428.
- Arsic, N, Zaccagna, S, Zentilin, L, Ramirez-Correa, G, Pattarini, L, Salvi, A *et al.* (2004). Vascular endothelial growth factor stimulates skeletal muscle regeneration in vivo. *Mol Ther* **10**: 844–854.
- De Coppi, P, Delo, D, Farrugia, L, Udomypanyan, K, Yoo, JJ, Nomi, M *et al.* (2005). Angiogenic gene-modified muscle cells for enhancement of tissue formation. *Tissue Eng* **11**: 1034–1044.
- Levenberg, S, Rouwkema, J, Macdonald, M, Garfein, ES, Kohane, DS, Darland, DC *et al.* (2005). Engineering vascularized skeletal muscle tissue. *Nat Biotechnol* **23**: 879–884.
- Gregorevic, P, Blankinship, MJ, Allen, JM, Crawford, RW, Meuse, L, Miller, DG *et al.* (2004). Systemic delivery of genes to striated muscles using adeno-associated viral vectors. *Nat Med* **10**: 828–834.
- Partridge, TA, Morgan, JE, Coulton, GR, Hoffman, EP and Kunkel, LM (1989). Conversion of mdx myofibers from dystrophin-negative to -positive by injection of normal myoblasts. *Nature* **337**: 176–179.
- Huard, J, Acsadi, G, Jani, A, Massie, B and Karpati, G (1994). Gene transfer into skeletal muscles by isogenic myoblasts. *Hum Gene Ther* **5**: 949–958.
- Gussoni, E, Soneoka, Y, Strickland, CD, Buzney, EA, Khan, MK, Flint, AF *et al.* (1999). Dystrophin expression in the mdx mouse restored by stem cell transplantation. *Nature* **401**: 390–394.
- Kinoshita, I, Vilquin, JT, Guérette, B, Asselin, I, Roy, R and Tremblay, JP (1994). Very efficient myoblast allotransplantation in mice under FK506 immunosuppression. *Muscle Nerve* **17**: 1407–1415.
- Vilquin, JT, Wagner, E, Kinoshita, I, Roy, R and Tremblay, JP (1995). Successful histocompatible myoblast transplantation in dystrophin-deficient mdx mouse despite the production of antibodies against dystrophin. *J Cell Biol* **131**: 975–988.
- Qu-Petersen, Z, Deasy, B, Jankowski, R, Ikezawa, M, Cummins, J, Pruchnic, R *et al.* (2002). Identification of a novel population of muscle stem cells in mice: potential for muscle regeneration. *J Cell Biol* **157**: 851–864.
- Deasy, BM, Gharaibeh, BM, Pollett, JB, Jones, MM, Lucas, MA, Kanda, Y *et al.* (2005). Long-term self-renewal of postnatal muscle-derived stem cells. *Mol Biol Cell* **16**: 3323–3333.
- Tamaki, T, Uchiyama, Y, Okada, Y, Ishikawa, T, Sato, M, Akatsuka, A *et al.* (2005). Functional recovery of damaged skeletal muscle through synchronized vasculogenesis, myogenesis, and neurogenesis by muscle-derived stem cells. *Circulation* **112**: 2857–2866.
- Peng, H, Usas, A, Olshanski, A, Ho, AM, Gearhart, B, Cooper, GM *et al.* (2005). VEGF improves, whereas sFlt1 inhibits, BMP2-induced bone formation and bone healing through modulation of angiogenesis. *J Bone Miner Res* **20**: 2017–2027.
- Peng, H, Wright, V, Usas, A, Gearhart, B, Shen, HC, Cummins, J *et al.* (2002). Synergistic enhancement of bone formation and healing by stem cell-expressed VEGF and bone morphogenetic protein-4. *J Clin Invest* **110**: 751–759.
- Payne, TR, Oshima, H, Okada, M, Momi, N, Tobita, K, Keller, BB *et al.* (2007). A relationship between vascular endothelial growth factor, angiogenesis, and cardiac

- repair after muscle stem cell transplantation into ischemic hearts. *J Am Coll Cardiol* **50**: 1677–1684.
24. Deasy, BM, Qu-Peterson, Z, Greenberger, JS and Huard, J (2002). Mechanisms of muscle stem cell expansion with cytokines. *Stem Cells* **20**: 50–60.
  25. Schmidt, BT, Feduska, JM, Witt, AM and Deasy BM (2008). Robotic cell culture system for stem cell assays. *Ind Robot Int J* **35**: 116–124.
  26. Deasy, BM, Jankowski, RJ, Payne, TR, Cao, B, Goff, JP, Greenberger, JS *et al.* (2003). Modeling stem cell population growth: incorporating terms for proliferative heterogeneity. *Stem Cells* **21**: 536–545.
  27. Horak, ER, Leek, R, Klenk, N, Lejeune, S, Smith, K, Stuart, N *et al.* (1992). Angiogenesis, assessed by platelet/endothelial cell adhesion molecule antibodies, as indicator of node metastases and survival in breast cancer. *Lancet* **340**: 1120–1124.
  28. Albelda, SM, Muller, WA, Buck, CA and Newman, PJ (1991). Molecular and cellular properties of PECAM-1 (endoCAM/CD31): a novel vascular cell-cell adhesion molecule. *J Cell Biol* **114**: 1059–1068.
  29. Springer, ML, Chen, AS, Kraft, PE, Bednarski, M and Blau, HM (1998). VEGF gene delivery to muscle: potential role for vasculogenesis in adults. *Mol Cell* **2**: 549–558.
  30. Springer, ML, Ozawa, CR, Banfi, A, Kraft, PE, Ip, TK, Brazelton, TR *et al.* (2003). Localized arteriole formation directly adjacent to the site of VEGF-induced angiogenesis in muscle. *Mol Ther* **7**: 441–449.
  31. Lee, JY, Qu-Petersen, Z, Cao, B, Kimura, S, Jankowski, R, Cummins, J *et al.* (2000). Clonal isolation of muscle-derived cells capable of enhancing muscle regeneration and bone healing. *J Cell Biol* **150**: 1085–1100.
  32. Dellavalle, A, Sampaolesi, M, Tonlorenzi, R, Tagliafico, E, Sacchetti, B, Perani, L *et al.* (2007). Pericytes of human skeletal muscle are myogenic precursors distinct from satellite cells. *Nat Cell Biol* **9**: 255–267.
  33. Taviani, M, Zheng, B, Oberlin, E, Crisan, M, Sun, B, Huard, J *et al.* (2005). The vascular wall as a source of stem cells. *Ann N Y Acad Sci* **1044**: 41–50.
  34. Crisan, M, Yap, S, Casteilla, L, Chen, CW, Corselli, M, Park, TS *et al.* (2008). A perivascular origin for mesenchymal stem cells in multiple human organs. *Cell Stem Cell* **3**: 301–313.
  35. Zheng, B, Cao, B, Crisan, M, Sun, B, Li, G, Logar, A *et al.* (2007). Prospective identification of myogenic endothelial cells in human skeletal muscle. *Nat Biotechnol* **25**: 1025–1034.
  36. Urish, K, Kanda, Y and Huard, J (2005). Initial failure in myoblast transplantation therapy has led the way toward the isolation of muscle stem cells: potential for tissue regeneration. *Curr Top Dev Biol* **68**: 263–280.
  37. Ozawa, CR, Banfi, A, Glazer, NL, Thurston, G, Springer, ML, Kraft, PE *et al.* (2004). Microenvironmental VEGF concentration, not total dose, determines a threshold between normal and aberrant angiogenesis. *J Clin Invest* **113**: 516–527.
  38. Karpati, G, Carpenter, S and Prescott, S (1988). Small-caliber skeletal muscle fibers do not suffer necrosis in mdx mouse dystrophy. *Muscle Nerve* **11**: 795–803.
  39. Okano, T, Yoshida, K, Nakamura, A, Sasazawa, F, Oide, T, Takeda, S *et al.* (2005). Chronic exercise accelerates the degeneration-regeneration cycle and downregulates insulin-like growth factor-1 in muscle of mdx mice. *Muscle Nerve* **32**: 191–199.
  40. Bouchentouf, M, Benabdallah, BF, Bigey, P, Yau, TM, Scherman, D and Tremblay, JP (2008). Vascular endothelial growth factor reduced hypoxia-induced death of human myoblasts and improved their engraftment in mouse muscles. *Gene Ther* **15**: 404–414.
  41. Delo, DM, Eberli, D, Williams, JK, Andersson, KE, Atala, A and Soker, S (2008). Angiogenic gene modification of skeletal muscle cells to compensate for ageing-induced decline in bioengineered functional muscle tissue. *BJU Int* **102**: 878–884.
  42. Jankowski, RJ, Deasy, BM, Cao, B, Gates, C and Huard, J (2002). The role of CD34 expression and cellular fusion in the regeneration capacity of myogenic progenitor cells. *J Cell Sci* **115**(Pt 22): 4361–4374.